

Low-Energy Precision Physics and Lattice QCD

**B. B. Brandt¹, A. Francis², V. Gülpers^{2,3}, G. Herdoiza³, G. von Hippel³, H. Horch³,
B. Jäger^{2,3}, H. B. Meyer^{2,3}, T. Rae³, and H. Wittig^{2,3}**

¹ Institut für Theoretische Physik, Universität Regensburg, 93040 Regensburg, Germany

² Helmholtz Institute Mainz, Johannes Gutenberg-Universität Mainz, 55099 Mainz, Germany

³ PRISMA Cluster of Excellence and Institut für Kernphysik,
Johannes Gutenberg-Universität Mainz, 55099 Mainz, Germany
E-mail: wittig@kph.uni-mainz.de

We present results for pion and nucleon form factors, as well as the hadronic vacuum polarisation contribution to the muon ($g - 2$) obtained from lattice QCD. By using $O(a)$ improved Wilson quarks for near-physical pion masses and three values of the lattice spacing we achieve good control over systematic errors associated with lattice artefacts and extrapolations to the physical pion mass. Several technical improvements are discussed, including the efficient calculation of quark-disconnected diagrams, the reduction of unwanted excited-state contributions in baryonic correlation functions, and the impact of using partially twisted boundary conditions.

1 Introduction

Lattice QCD has emerged as a versatile tool for tackling a wide range of topics in strong interaction physics. Lattice calculations of the light hadron spectrum have contributed significantly to validating QCD as the theory of the strong interaction. Furthermore, lattice QCD makes precise predictions for Standard Model parameters, such as quark masses and the strong coupling constant, as well as for mesonic decay constants and form factors, which are relevant for obtaining accurate estimates of the elements of the Cabibbo-Kobayashi-Maskawa matrix. These successes have established lattice QCD as a mature field, whose status is further underlined by the fact that an international collaboration is now preparing global averages of lattice results, very much in the spirit of the Particle Data Group¹.

Lattice calculations are also increasingly important for the interpretation of experimental results on hadron structure and tests of the Standard Model². In this contribution we report on our results for form factors of the pion and the nucleon, as well as on the hadronic vacuum polarisation contribution to the muon's anomalous magnetic moment. As will become clear, there are several technical issues which must be addressed before the overall accuracy of these quantities can be claimed to be comparable or even better than what can be achieved in other phenomenological approaches.

2 Hadron Structure on the Lattice

The internal structure of hadrons has been the subject of a major experimental programme at accelerator facilities worldwide, which must be matched by equally precise theoretical analyses. In particular, one wants to gain a quantitative understanding of structural properties of the nucleon in terms of QCD. To this end, one confronts precise measurements of form factors and structure functions to the corresponding predictions of the theory. Lattice

calculations of baryonic observables are technically much more difficult compared to their mesonic counterparts. Therefore, quantities such as pion form factors offer an ideal testing ground for state-of-the-art lattice methods before they are applied in the baryonic sector.

Chiral Perturbation Theory (χ PT) is another theoretical tool for studying the strong interaction at low energies. While lattice QCD seeks to describe hadronic properties in terms of the fundamental constituents, i.e. quarks and gluons, χ PT is an effective theory based on hadronic degrees of freedom. Lattice QCD and χ PT complement each other: on the one hand, lattice simulations are typically performed at unphysically large light-quark masses and thus χ PT is used to extrapolate lattice data to the physical point; on the other hand, lattice simulations allow one to compute matrix elements that can also be calculated in χ PT, and thus to determine the low-energy parameters of χ PT from first principles.

2.1 The Electromagnetic and Scalar Form Factors of the Pion

The pion – the lightest bound-state in the spectrum of QCD – is best suited to perform a matching between lattice QCD and χ PT. The non-perturbative phenomena governing the structure of hadrons is encoded in form factors depending on the momentum transfer Q^2 . While the *electromagnetic* form factor of the pion provides information on the distribution of its charged constituents, namely valence and sea light quarks, the *scalar* form factor of the pion describes the coupling of the pion to the Higgs boson.

A comprehensive account of our study of the pion electromagnetic form factor has recently been published³. Here, we briefly report on the most salient aspects of this work. Ensembles generated by the CLS initiative with two dynamical flavours of non-perturbatively $O(a)$ -improved Wilson fermions were used. The computation was performed at three different values of the lattice spacing in the range 0.05 – 0.08 fm and pion masses between 280 and 630 MeV at $m_\pi L \geq 4$. The use of partially twisted boundary conditions^{4,5} has allowed for a determination of the form factor with a very fine resolution of the momentum dependence. Fig. 1 shows a comparison of our results from two ensembles, corresponding to $m_\pi = 325$ MeV and 280 MeV, to determinations from other lattice collaborations and

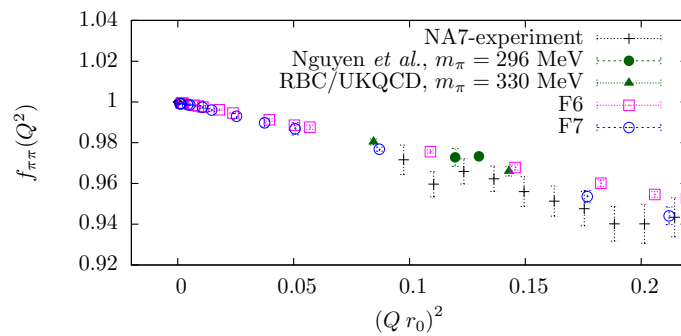


Figure 1. Compilation of results for the pion electromagnetic form factor in dynamical lattice QCD and as determined from experiment. Our measurements are labelled by the name on the ensembles, F6 and F7, corresponding to $m_\pi = 325$ MeV and 280 MeV, respectively. We achieve a high density of points in the immediate vicinity of $Q^2 = 0$ thanks to the use of twisted boundary conditions.

from experiment. The dense set of data points near vanishing momentum transfer allows for a precise and model-independent determination of the pion’s charge radius $\langle r_\pi^2 \rangle$ from the slope of $f_{\pi\pi}(Q^2)$ at $Q^2 = 0$.

In order to better constrain the mass and Q^2 -dependence of the pion form factor, it is useful to perform simultaneous fits to the form factor, the pion decay constant and the pion mass, based on the expressions of χ PT. We then observe that χ PT at next-to-leading-order (NLO) fails to produce a consistent description of our lattice data for the entire set of pion observables in the studied mass range $m_\pi \geq 280$ MeV. While individual fits to the pion mass and the pion decay constant lead to a coherent picture, inconsistencies arise when data for the form factor are included as well. By contrast, the NNLO expressions allow for a fully consistent description of all three observables, at the current statistical precision. The resulting estimate for the charge radius at the physical pion mass reads³

$$\langle r_\pi^2 \rangle = 0.481(33)(13) \text{ fm}^2, \quad (1)$$

the first error is statistical, while the second is an estimate of the total systematic uncertainty. This estimate is in very good agreement with the result $\langle r_\pi^2 \rangle = 0.452(11) \text{ fm}^2$ quoted by the PDG⁶.

The correlation function relevant for the determination of the *scalar* form factor of the pion receives contributions from quark-disconnected diagrams, which are notoriously difficult to evaluate with good statistical accuracy. Several techniques have been developed to address this challenging computation. In our recent analysis⁷ we have employed stochastic all-to-all propagators in combination with a hopping parameter expansion⁸, in order to evaluate the disconnected contribution. Our findings indicate that the contribution from disconnected diagrams is far from being negligible, particularly so, near the physical pion mass. This is illustrated in Fig. 2 for the case of the pion scalar radius, which is related to

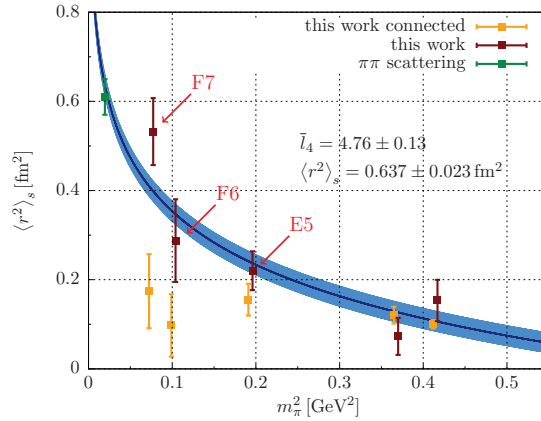


Figure 2. The scalar radius of the pion plotted against the pion mass squared. Dark red points denote the results obtained from the full (i.e. connected and disconnected) contributions, while yellow points represent the connected contribution only. Labels denote the ensembles computed on JUQUEEN. We observe that the contribution from disconnected diagrams is far from being negligible, particularly so, near the physical pion mass.

the derivative of the form factor at $Q^2 = 0$. After performing a chiral extrapolation to the physical pion mass, based on χ PT at NLO, we find

$$\langle r_\pi^2 \rangle_s = 0.637(23) \text{ fm}^2, \quad (2)$$

where the error is statistical. We stress that this estimate is consistent with a phenomenological determination based on $\pi\pi$ scattering⁹, but only after including the disconnected contribution.

2.2 Nucleon Structure

Lattice QCD has produced an impressive collection of phenomenologically relevant results for masses and decay properties of hadrons. However, the picture for many hadron structure observables of the nucleon – such as the nucleon axial charge g_A or the momentum fraction $\langle x \rangle_{u-d}$ – is somewhat less satisfactory. Moreover, the Q^2 -dependence of isovector electromagnetic form factors of the nucleon obtained in lattice calculations mostly disagrees with the experimental findings^{10,11}. Furthermore, calculations of the nucleon axial charge, g_A , tend to underestimate this quantity by typically 10 – 15%. There is a broad consensus that systematic effects are non-negligible for these quantities.

Among the common sources of systematic error are lattice artefacts and the influence of finite-volume effects. An obvious question is whether the chiral behaviour is sufficiently controlled in the calculations performed so far, or whether much smaller pion masses are required in order to make contact with the experimental value. One major issue addressed by our group^{12,13} is the possible contamination of the ground state of correlation functions by contributions from higher excited states. This is particularly problematic for baryon correlation functions, since their bad signal-to-noise ratio does not allow for long Euclidean time separations between the interpolating operators and local currents and densities. To address this issue, our group has advocated the use of “summed operator insertions”¹⁴, in which excited state contributions are parametrically more strongly suppressed compared to the conventional ratios of correlation functions.

The construction of interpolating operators which maximise the overlap with the ground state in correlation functions is crucial for any effort to address the issue of excited states contamination. Source smearing is widely used in order to create operators with improved projection properties. The intuition behind this is that a hadron should be best described by a state created by a spatially extended operator rather than a point-like one, guided by the principle that the spatial profile of the extended operator resembles the shape of the hadron in question. We have recently proposed new types of smearing which allow to achieve a reduction in the noise-to-signal ratio in correlation functions at non-zero momentum¹⁵ or to preserve the shape of the smearing function when performing the continuum-limit extrapolation¹⁶.

Overall, significant progress in addressing the systematic effects present in the quantities related to baryon structure has been achieved over the last few years. In Fig. 3 the pion mass dependence of g_A obtained from summed insertions is compared to the conventional method. The summation method clearly produces estimates in much better agreement with experiment. A chiral extrapolation of our results to the physical pion mass yields¹³

$$g_A = 1.223(63)_{(-60)}^{(+35)} \quad (3)$$

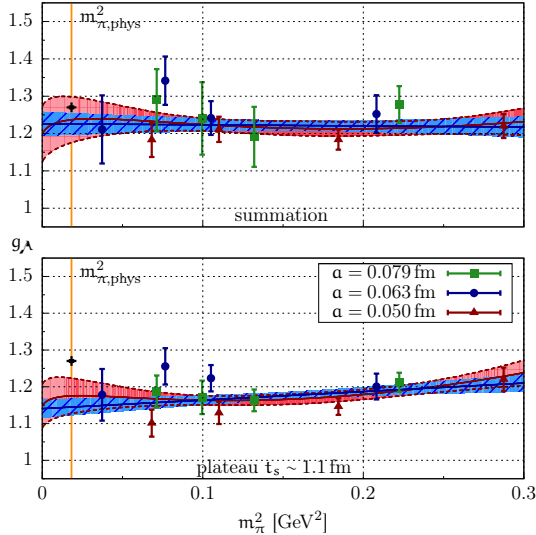


Figure 3. Pion mass dependence of the axial charge g_A obtained from summed insertions (upper panel) and the conventional plateau method (lower panel). The blue and red band represent different model functions for the chiral extrapolation. The left-most point denotes the experimental value.

the first error is statistical. This compares very well with the experimental determination of $g_A = 1.2701(25)^6$. Our study has revealed that the agreement between experiment and lattice data for g_A can be substantially improved when excited state contributions are properly taken into account.

3 Hadronic Contribution to the Anomalous Magnetic Moment of the Muon

The magnetic moment of a charged lepton is extracted from the vertex function describing the interaction between the lepton and a photon in the limit of vanishing photon momentum. The corresponding anomalous magnetic moment a_l is then defined as half the difference between the gyromagnetic factor g and its classical value of 2, i. e. $a_l = (g_l - 2)/2$. In the case of the electron, the quantity is dominated by QED contributions. The anomalous magnetic moment mediates helicity flip transitions, which implies that quantum corrections due to heavier particles of mass M , in the Standard Model or beyond, are proportional to m_l^2/M^2 . For this reason the muon anomalous magnetic moment a_μ is regarded as a sensitive probe for effects of nearby New Physics. However, by the same argument, given that $m_\mu \leq m_\pi$, the hadronic contributions to a_μ are larger and notoriously difficult to quantify.

While the experimental and theoretical estimates have both reached similar levels of precision of 0.5 ppm, a tension by 2 or 3 standard deviations between theory and experiment persists. Before invoking “new physics” as the reason for this tension the theoretical result and, in particular, all contributions due to hadronic effects, must be corroborated.

The uncertainty is dominated mainly by the leading order hadronic vacuum polarisation contribution a_μ^{HVP} and secondly by the hadronic light-by-light contributions. Currently a_μ^{HVP} is estimated via a phenomenological approach based on the evaluation of a dispersion integral. In the low-energy regime, the spectral function in the integrand must be determined experimentally, either from the cross section $e^+e^- \rightarrow \text{hadrons}$ or from the rate of hadronic τ -decays. Despite the different systematics, both methods produce results in broad agreement, provided that isospin breaking effects are properly accounted for¹⁷. None of them, however, reduces the discrepancy between theory and experiment on a_μ . A purely theoretical estimate of a_μ^{HVP} from a first-principles approach is clearly desirable. Our group has pursued a research programme¹⁸ aiming at an accurate determination of a_μ^{HVP} using lattice QCD.

In the lattice approach, the hadronic vacuum polarisation contribution to $(g-2)_\mu$ is determined by a convolution integral

$$a_\mu^{\text{HVP}} = 4\alpha^2 \int_0^\infty F(Q^2) (\Pi(0) - \Pi(Q^2)) dQ^2, \quad (4)$$

where $\Pi(Q^2)$ is the vacuum polarisation function (VPF) computed on the lattice from the Fourier transform of the current-current correlator. The kernel $F(Q^2)$ is a known analytic function, and α is the fine-structure constant. An important ingredient in our approach is the use of partially twisted boundary condition, in order to enhance the Q^2 -resolution near the origin. This is crucial for the determination of the additive contribution, $\Pi(0)$, which enters the convolution integral. Fig. 4 shows the VPF measured on an ensemble with our lowest pion mass, $m_\pi \approx 190$ MeV, satisfying $L \approx 4$ fm. By comparing the Q^2 -position and the number of red and blue data points, corresponding to periodic and twisted boundary conditions, respectively, one clearly observes the advantages provided by the lat-

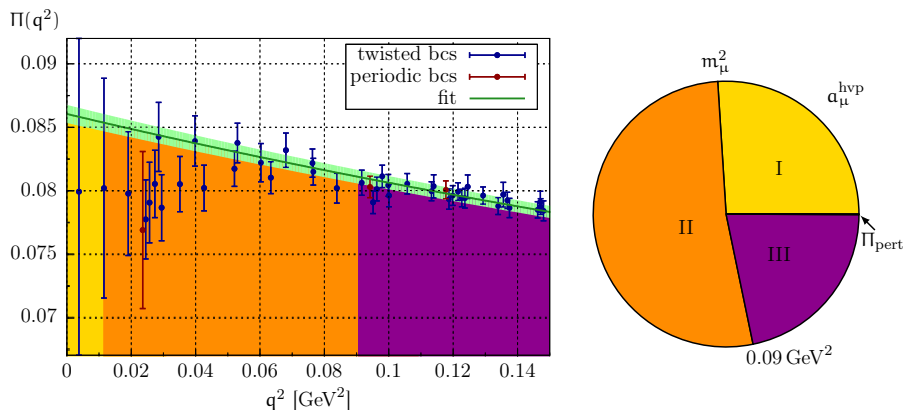


Figure 4. Momentum dependence of the vacuum polarisation with periodic and twisted boundary conditions shown for an ensemble with $m_\pi \sim 190$ MeV, $L \sim 4$ fm and a lattice spacing $a = 0.063$ fm. The different momentum ranges have been separated by different colours.

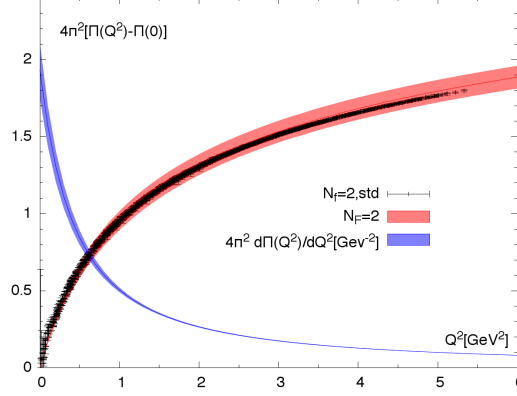


Figure 5. The subtracted vacuum polarisation $\widehat{\Pi}(Q^2) = \Pi(Q^2) - \Pi(0)$ and the Adler function $d\widehat{\Pi}(Q^2)/dQ^2$ using the recently proposed time-momentum method (coloured bands). The data shown in black were obtained using the standard momentum-space method.

ter choice. This figure also indicates the importance of reaching the small Q^2 regime and, in particular, the left-most yellow region corresponding to $Q^2 \leq m_\mu^2$, where the integrand in Eq. 4 is peaked. The right panel of Fig. 4 shows the relative contribution from data in different Q^2 intervals.

In order to obtain an accurate lattice estimate of a_μ^{HVP} further attempts are necessary to achieve good control of the low- Q^2 region. We have recently tested¹⁹ an alternative method²⁰ based on the time-momentum representation of the vector-vector correlator, in which Q^2 is a tunable parameter. Preliminary results are shown in Fig. 5, where they are compared to the standard method on the same ensembles. We expect that by combining the two methods by which we have computed the VPF, a significant improvement in the determination of a_μ^{HVP} can eventually be achieved.

4 Conclusion

Lattice QCD calculations are increasingly important for the interpretation of experimental results on hadron structure and for constraining the limits of the Standard Model. In this contribution we have presented a status report of our ongoing projects aimed at determining hadronic form factors and the leading-order hadronic vacuum polarisation contribution to the muon ($g - 2$) with high precision. Currently, efforts are still focused on controlling various sources of systematic error, such as excited state contamination, contributions from disconnected diagrams, or the uncertainty associated with the small-momentum region. It is expected that the technical improvements discussed above will soon allow for determinations of these quantities with the accuracy required for having a big impact on phenomenological studies.

Acknowledgements

Our simulations were performed on JUQUEEN and JUROPA as part of NIC project HMZ21, and on the dedicated QCD cluster “Wilson” at the Institute for Nuclear Physics, University of Mainz. We thank Dalibor Djukanovic and Christian Seiwerth for technical support.

References

1. G. Colangelo *et al.*, Eur. Phys. J. C **71** (2011) 1695 arXiv:1011.4408 [hep-lat].
2. H. Wittig, Mod. Phys. Lett. A **28** (2013) 1.
3. B. B. Brandt, A. Jüttner and H. Wittig, arXiv:1306.2916 [hep-lat].
4. G. M. de Divitiis, R. Petronzio and N. Tantalo, Phys. Lett. B **595** (2004) 408, hep-lat/0405002.
5. C. T. Sachrajda and G. Villadoro, Phys. Lett. B **609** (2005) 73, hep-lat/0411033.
6. J. Beringer *et al.* [Particle Data Group Collaboration], Phys. Rev. D **86** (2012) 010001.
7. V. Gülpers, G. von Hippel and H. Wittig, arXiv:1309.2104 [hep-lat].
8. G. S. Bali, S. Collins and A. Schafer, Comput. Phys. Commun. **181** (2010) 1570 arXiv:0910.3970 [hep-lat].
9. G. Colangelo, J. Gasser and H. Leutwyler, Nucl. Phys. B **603** (2001) 125 [hep-ph/0103088].
10. C. Alexandrou, PoS LATTICE **2010** (2010) 001, arXiv:1011.3660 [hep-lat].
11. H.-W. Lin, PoS LATTICE **2012** (2012) 013, arXiv:1212.6849 [hep-lat].
12. S. Capitani, B. Knippschild, M. Della Morte and H. Wittig, PoS LATTICE **2010** (2010) 147 arXiv:1011.1358 [hep-lat].
13. S. Capitani, M. Della Morte, G. von Hippel, B. Jäger, A. Jüttner, B. Knippschild, H. B. Meyer and H. Wittig, Phys. Rev. D **86** (2012) 074502, arXiv:1205.0180.
14. L. Maiani, G. Martinelli, M. L. Paciello and B. Taglienti, Nucl. Phys. **B293** (1987) 420.
15. M. Della Morte, B. Jäger, T. Rae and H. Wittig, Eur. Phys. J. A **48** (2012) 139 arXiv:1208.0189 [hep-lat].
16. G. M. von Hippel, B. Jäger, T. D. Rae and H. Wittig, JHEP **1309** (2013) 014, arXiv:1306.1440 [hep-lat].
17. F. Jegerlehner and R. Szafron, Eur. Phys. J. C **71** (2011) 1632 arXiv:1101.2872 [hep-ph].
18. M. Della Morte, B. Jäger, A. Jüttner and H. Wittig, JHEP **1203** (2012) 055 arXiv:1112.2894 [hep-lat].
19. A. Francis, B. Jäger, H. B. Meyer and H. Wittig, Phys. Rev. D **88** (2013) 054502, arXiv:1306.2532 [hep-lat].
20. D. Bernecker and H. B. Meyer, Eur. Phys. J. A **47** (2011) 148, arXiv:1107.4388 [hep-lat].